PHOTONIC SENSORS / Vol. 7, No. 2, 2017: 123–130

Alcohol Sensing Over O+E+S+C+L+U Transmission Band Based on Porous Cored Octagonal Photonic Crystal Fiber

Bikash Kumar PAUL[1, 2], Md. Shadidul ISLAM[1], Kawsar AHMED[1,2*], and Sayed ASADUZZAMAN[1,2,3]

[1]*Department of Information and Communication Technology, Mawlana Bhashani Science and Technology University Santosh, Tangail-1902, Bangladesh*

[2]*Group of Bio-Photomatriχ, Tangail-1902, Bangladesh*

[3]*Department of Software Engineering, Daffodil International University, Sukrabad, Dhaka, Bangladesh*

[*]Corresponding author: Kawsar AHMED E-mail: kawsar.ict@mbstu.ac.bd and k.ahmed.bd@ieee.org

Abstract: A micro structure porous cored octagonal photonic crystal fiber (P-OPCF) has been proposed to sense aqueous analysts (alcohol series) over a wavelength range of 0.80 μm to 2.0 μm. By implementing a full vectorial finite element method (FEM), the numerical simulation on the proposed O-PCF has been analyzed. Numerical investigation shows that high sensitivity can be gained by changing the structural parameters. The obtained result shows the sensitivities of 66.78%, 67.66%, 68.34%, 68.72%, and 69.09%, and the confinement losses of 2.42×10^{-10} dB/m, 3.28×10^{-11} dB/m, 1.21×10^{-6} dB/m, 4.79×10^{-10} dB/m, and 4.99×10^{-9} dB/m at the 1.33 μm wavelength for methanol, ethanol, propanol, butanol, and pentanol, respectively can satisfy the condition of much legibility to install an optical system. The effects of the varying core and cladding diameters, pitch distance, operating wavelength, and effective refractive index are also reported here. It reflects that a significant sensitivity and low confinement loss can be achieved by the proposed P-OPCF. The proposed P-OPCF also covers the wavelength band (O+E+S+C+L+U). The investigation also exhibits that the sensitivity increases when the wavelength increases like $S_{\text{O-band}}<S_{\text{E-band}}<S_{\text{S-band}}<S_{\text{C-band}}<S_{\text{L-band}}<S_{\text{U-band}}$. This research observation has much pellucidity which has remarkable impact on the field of optical fiber sensor.

Keywords: Porous cored OPCF; alcohol sensor; sensitivity; confinement loss; transmission band

Citation: Bikash Kumar PAUL, Md. Shadidul ISLAM1, Kawsar AHMED, and Sayed ASADUZZAMAN, "Alcohol Sensingover O+E+S+C+L+U Transmission Band Based on Porous Cored Octagonal Photonic Crystal Fiber," *Photonic Sensors*, 2017, 7(2): 123–130.

1. Introduction

A massive technological change emerges through the innovative invention of researchers. As an optical medium, photonic crystal has some identical properties [1–11]. The photonic crystal fibers are enormously used in the optical fiber technology due to its idiosyncratic properties. In 1996, Knight *et al.* firstly proposed the photonic crystal fiber for its novel competence [11]. The photonic crystal fiber is a fiber in which artificial frequent capillaries occur. Optical characteristics are mainly controlled by the number and size or magnitude of microstructure capillaries of air holes [12] and various structural diversities. Photonic crystal fibers (PCF) are becoming more and more

Received: 5 September 2016 / Revised: 30 November 2016

DOI: 10.1007/s13320-017-0376-6
Article type: Regular

popular for its better guiding properties, robustness, and flexibility.

Some identical properties are seen like as nonlinearity [1, 2], high birefringence [3, 4], high sensitivity [5, 6], low confinement loss [7, 8], improved effective area, and endlessly single mode [9–11]. For these reasons, PCF has drawn a great attraction among researchers. At the beginning time, PCF has limited applications areas. Now PCF is used in fields of THz telecommunications [13], nonlinear optics [14], bio sensing [15], chemical sensing [16, 17], spectroscopy [18], optical chromatography [19], and fuel adulteration detection [20]. In medical science, it is becoming more and more popular for bio-photonics [21] and neuro-photonics [22]. It is also used in the fields of cancer cell detection, HIV viral load detection [23], protein detection [24], diabetics detection [25], etc. Different types of PCF are used for numerous applications for their superb guiding capability.

As a novel method, optical indexed guiding PCF is well rebounded [26]. Depending on the light guiding mechanism process, a crystal fiber PCF can be categorized into two classes. One is the photonic band gap fiber which uses the photonic band gap (PBG) effect for guiding light through that fiber thus it is called PBG-PCF. The other one uses common optical properties total internal reflection (TIR) thus it is called TIR-PCF. PCFs are formed by the crystal which is made of silica glass. The main reason for choosing silica glass as a background material is its paramount property which provides momentous amenities. Recently, graphene [27], chalconide glass with polymer [28], telluride, and topus [29] are also used to fabricate PCF.

The first proposal of PCF came from Yeh *et al.* in 1978 [30]. But a photonic crystal fiber was designed using two-dimensional (2D) photonic crystals by Russel [31]. This fiber consisted of single air core, which was reported in Optical Fiber Conference at San Jose, CA in 1996 [32]. As a consequence in 1997, endlessly single mode fiber was invented. Highly birefringent PCF (HB-PCF) opened a new horizon in 2000. Later Bragg fiber, PCF laser, and PCF with ultra-flatted dispersion were invented. Recently, gas and liquid filled PCF created a new diversity in different application areas. In 2014, Ademgil proposed an octagonal PCF sensor for chemical sensing [26]. At operating the 1.00 μm wavelength, it shows approximately 47 % sensitivity for aqueous analytes. In 2015, Ahmed *et al.* designed an O-PCF which gives the indication of relatively high sensitivity [33].

In this paper, we propound a design and numerical analysis of microstructure circular porous core PCF with high sensitivity and low confinement for chemical sensing applications covering the O+S+C+L+U wavelength band. A five-layer octagonal air hole lattice array which acts as a cladding encompasses the core region. For electromagnetic computation, an anisotropic perfectly match layer (PML) plays a vital role in sensing performance. PML is also used in the proposed PCF to attenuate unwanted reflection of light wave [33]. Here PML acts as an absorbing layer. Variations of geometrical properties (parameters) are also examined to analyze the effects of guiding properties on P-OPCF.

2. Geometries of the proposed PCF

The transverse cross sectional view of the proposed P-OPCF is shown in Fig. 1(a). There are five rings in the designed structure in the cladding part, and each ring gives a view of an octagonal that's why it can be called as OPCF. For the first ring (the first layer) of the cladding, it contains 8 air holes. The number of air holes gets increased geometrically where the nearest next level number ring has 8 air holes more than the previous level of the ring. For the five rings, it can be represented as $8n$ where n is the number of levels, and the first ring is n=1 and will increase by 1 for each level until it touches the ring number five where total number of air hole is $8n$=8×5=40. Each air hole has the same

diameter where d=1.75 μm. The distance between two adjacent air holes of two conjugative rings is called pitch and denoted by Λ_1.

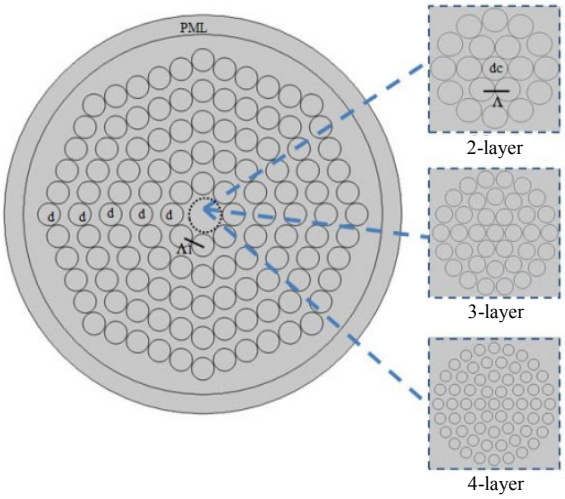

Fig. 1 Transverse cross-sectional view of the proposed P-OPCF.

The pivotal part of the proposed PCF contains a small area with two circular rings in porous shape which is known as core. Six holes filled with aqueous analysts are required to design the inner circle of the core where the outer circle has twelve holes filled. The core diameter d_c processes a very small area where d_c = 0.57 μm and each hole is filled with aqueous analysts that has the same diameter. The pitch of the core (Λ_c) is equal to Λ_c = 0.61 μm, and the two adjacent air holes are filled with aqueous analysts both in the same circle and between two circles. For two-layer circular porous core, the first layer has 6 holes in total which makes an angle of 60°, and the second layer has 12 holes which makes an angle of 30°. According to the sequence for three layers having 6, 12, and 18 holes, they make angles of 60°, 30°, and 20°, respectively. The four-layer porous core makes angles of 60°, 30°, 20°, and 15° for consequence layers, respectively.

The core cladding geometric structure is surrounded by anisotropic PML. Hence, we use a 10% of the PML size additive with an overall cladding size. The key component of the back ground, core, and cladding is pure silica where Sellmeier equation [35] is followed to determine the refractive index for the defined wavelength range.

3. Numerical analysis

A finite element method (FEM) is used to simulate our proposed photonic crystal fiber. The FEM sub-divides a larger complicated design into a smaller and simpler one which produces a more approximate solution. To design the issue of a PCF sensor, two fundamental parameters are directly associated.

The background material of the proposed P-OPCF is silica. As for the theoretical and experimental aspects, the refractive index (RI) is varying with wavelength λ for different materials. There is a relationship between the wavelength and RI of different transparent materials and liquids. Based on the relationship, an equation is derived which is highly used to determine RI of different crystals and liquids. This relationship was first found by Willhem Sellmeier in 1871. The equation is as follows:

$$n(\lambda)=\sqrt{1+\frac{B_1\lambda^2}{\lambda^2-C_1}+\frac{B_2\lambda^2}{\lambda^2-C_2}+\frac{B_3\lambda^2}{\lambda^2-C_3}} \quad (1)$$

where n and λ represent the refractive index and wavelength, respectively, and B_1, B_2, B_3, C_1, C_2, and C_3 are the coefficients of silica.

The effective refractive index can be calculated by

$$n_{\text{eff}}=B/k_0 \quad (2)$$

where B is the propagation constant, and $k_0 = 2\pi/\lambda$ is the free space wave number.

The sensitivity can be calculated by (3) which was reported in [33]:

$$r=\frac{n_r}{n_{\text{eff}}}f \quad (3)$$

where n_r is the RI of using materials within the air holes, and n_{eff} is the modal effective index. Here, f represents the percentage ratio between air hole power and total power which can be calculated by

$$f=\frac{\int_{\text{sample}}\text{Re}(E_xH_y-E_yH_x)dxdy}{\int_{\text{total}}\text{Re}(E_xH_y-E_yH_x)dxdy}\times 100 \quad (4)$$

where E_x and E_y are transverse and longitudinal electric fields, respectively, and H_x and H_y are transverse and longitudinal magnetic fields, respectively.

Light in the PCF should be confined into the core region. Due to the material impurity or structure combined, some light passes the outer of the core region, and the losses of light energy are treated as confinement losses or leakage losses. The loss can be calculated by using

$$L_c = 8.68 k_0 \, \mathrm{Im}[n_{\mathrm{eff}}] \tag{5}$$

where $\mathrm{Im}[n_{\mathrm{eff}}]$ is the imaginary part of the effective refractive index. Using the discussed equation above and FEM, a numerical result analysis is attained.

4. Result analysis

To construct a prognostic computational model for real world continuity numerous software use FEM. The accuracy of the computational model is directly involved with a numerical analysis. Different well-known numerical methods such as FEM, boundary element method (BEM), finite difference method (FDM), finite volume method (FVM), and mesh-less method (MLM) are used in the numerical computation. Among these numerical methods, FEM provides the most accurate computation. Along with FEM, the finer mesh analysis is used to gain more accurate solutions. By using the finer mesh analysis, we get 42294 elements (DOF degree of Freedom). COMSOL Multiphysics 4.2 has been used to investigate for the mesh and numerical analysis. According to the simulation result, Fig. 2 shows wavelength verses effective RI of our proposed optimized P-OPCF. It shows that the curves go downward due to an increase in the wavelength. This means that if we decrease the wavelength we get much higher effective RI and vice versa. This figure also represents the confinement of more light due to *X*-polarization and *Y*-Polarization at wavelength 1.33 μm for ethanol (n = 1.354).

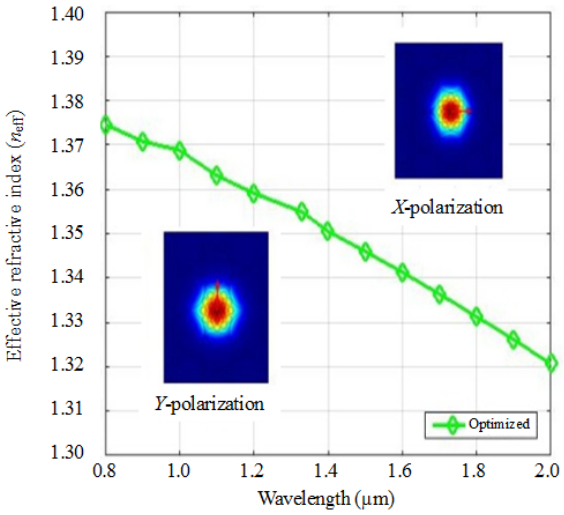

Fig. 2 Effective refractive index verses wavelength in *X*-polarization fundamental mode for optimized P-OPCF and n = 1.354.

Our desired goal is to getting much sensitivity and lower confinement loss, so we have investigated the core region by setting two, three, and four layers. Figure 3 shows the relative sensitivity verses wavelength for two-, three-, and four-layer porous core PCFs where two-layer core PCF is shown too much higher relative sensitivity than others. In addition, the confinement loss of 3.28×10^{-11} dB/m, 1.32×10^{-10} dB/m, and 6.96×10^{-11} dB/m for two, three, and four layers core respectively at the 1.33 μm wavelength for ethanol. Here the relative sensitivity of two-layer core is superior to others three- and four-layer core. Based on the above argument, we choose two-layer porous core O-PCF for the further investigation.

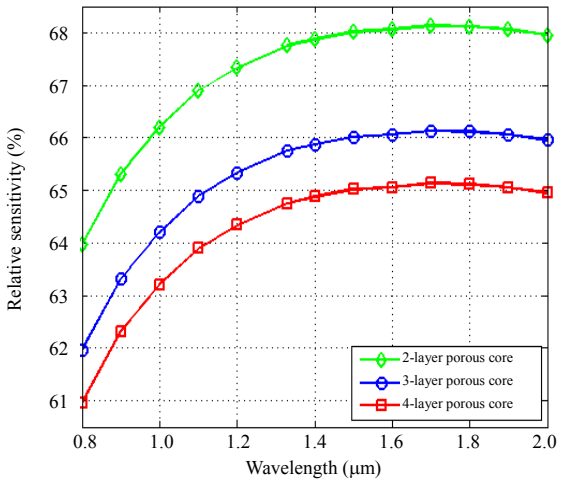

Fig. 3 Comparison of the relative sensitivity with core layer variations for n=1.354.

A fundamental factor confinement loss (CL) is a vital issue which should be remembered in mind at the fabrication time of PCF. To reduce the confinement loss of micro-structured P-OPCF is always desirable. For the confinement loss, some light energy encroaches into cladding area which must cause the main hindrance to the flow of informative light energy. Relative sensitivities of methanol, ethanol, propanol, butanol, and pentanolare are 66.78%, 67.66%, 68.34%, 68.72%, and 69.09 %, respectively at the 1.33 μm operating wavelength. Figure 4 depicts the relative sensitivity performance for alcohol analytes as methanol< ethanol< propanol< butanol< pentanol, respectively. It also exhibits that the sensitivity goes upward with an increase in the wavelength. Figure 5 shows the confinement losses for aqueous analysts of alcohol series methanol, ethanol, propanol, butanol, and pentanol, which are 2.42×10^{-10} dB/m, 3.28×10^{-11} dB/m, 1.21×10^{-6} dB/m, 4.79×10^{-10} dB/m, and 4.99×10^{-9} dB/m, respectively at the same wavelength.

Diameter/pitch (d/Λ), known as the air filling ratio, is tuned by modifying the core hole diameter and core pitch distance. Figure 6 shows that relative sensitivity curves are upward where in core region air filling ratio is high. So the air filling ratio has strong positive bonding with the relative sensitivity. We have investigated the relative sensitivity and confinement loss by varying the cladding air holes diameter which is shown in Figs. 7 and 8, respectively. It recounts comparatively higher sensitivity at d/Λ_1=0.931 and relatively lower sensitivity at d/Λ_1= 0.808 over the wavelength range 0.2 μm to 2.0 μm. To avoid fabrication tolerance, d/Λ_1= 0.931 is selected because that the maximum air filling ratio 0.94 is considerable for fabrication without any collapse [36].

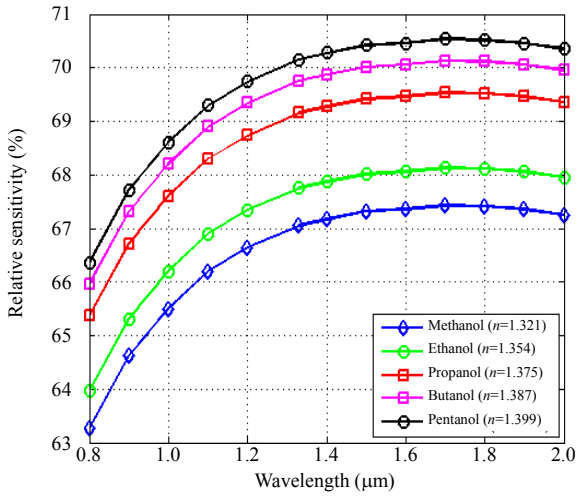

Fig. 4 Comparison of relative sensitivity with alcohol series for two-layer core.

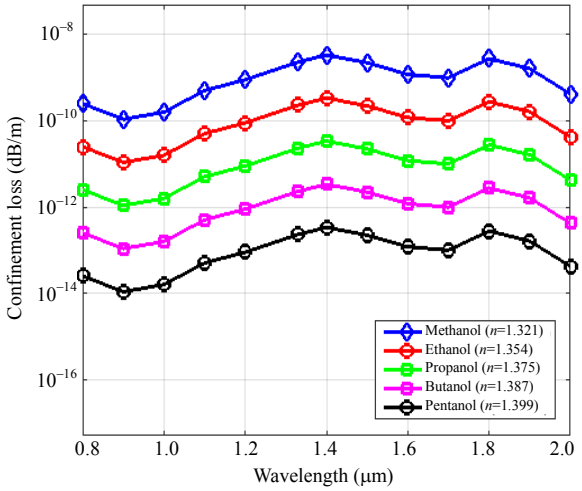

Fig. 5 Comparison of the confinement loss with alcohol series for two-layer core.

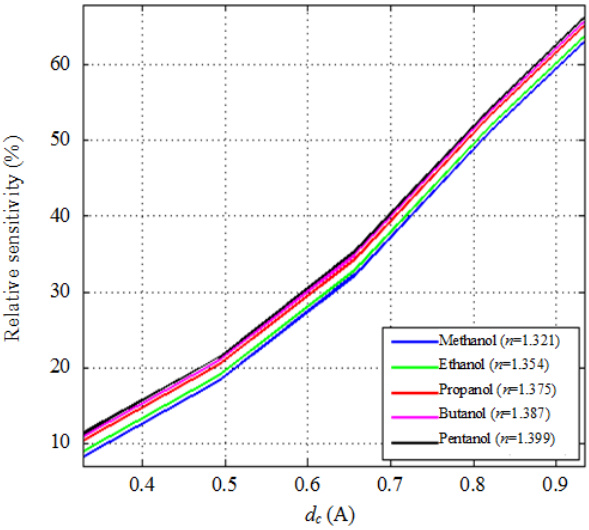

Fig. 6 Comparison of relative sensitivity with core air filling ratio (d_c/Λ) variations for alcohol series.

Fabrication is an important issue because expected characteristics of the proposed P-OPCF greatly depend on the fabrication accuracy. After the fabrication process, teeny change in parameters may

occur. For this unexpected error, we have changed different parameters of the proposed P-OPCF. At the time of fabrication, by using the standard draw there may occur ±1% variations on their overall parameters of PCF [38]. For this reason, we inspect the behaviors of the proposed P-OPCF by tuning the structural parameters in range from –2% to + 2%.

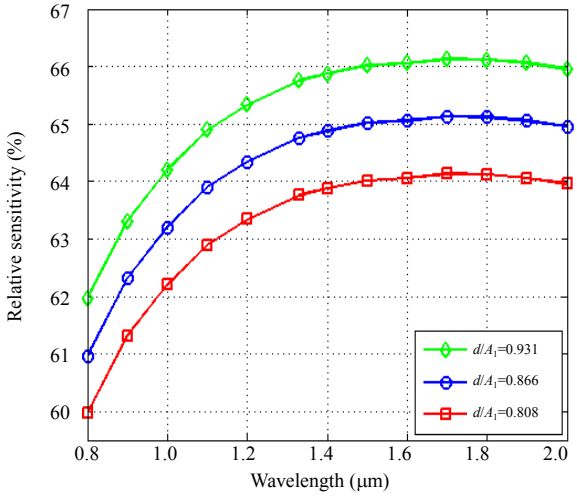

Fig. 7 Comparison of relative sensitivity with cladding air filling ratio (d/Λ_1) variations for n=1.354.

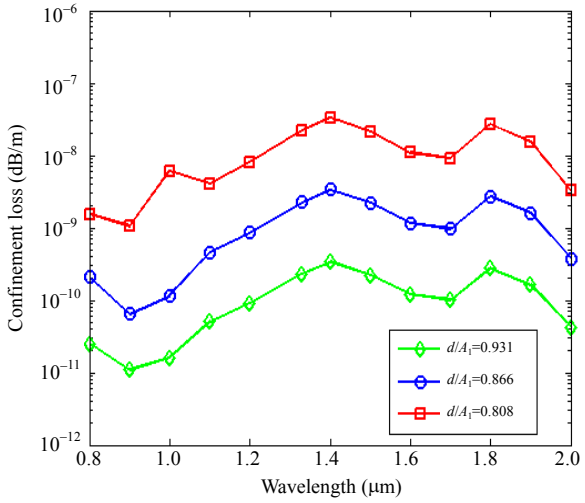

Fig.8 Comparison of confinement loss with cladding air filling ratio (d/Λ_1) variations for n = 1.354.

Figure 9 shows the inspection of wavelength verses the relative sensitivity, making –2%, –1%, +1%, and +2% variations with the optimum parameters. The simulation process goes down for a wider wavelength limit over 0.8 μm to 2.0 μm which does not make a great difference between the proposed P-OPCFs. By changing +2%, +1%, –1%, and –2% of overall parameters, the relative sensitivity as well as confinement loss is not affected greatly.

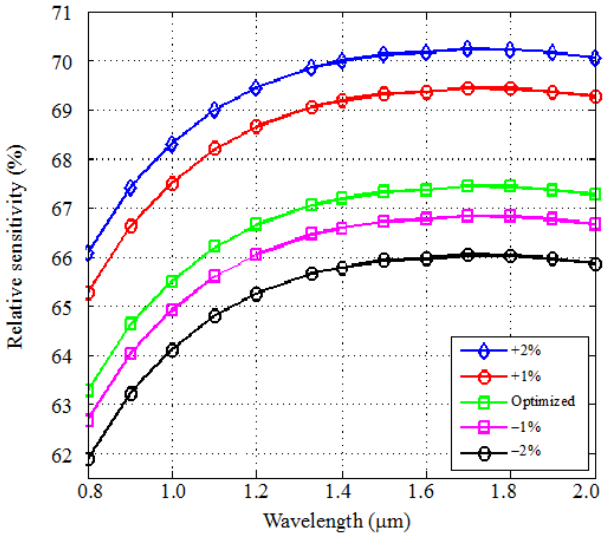

Fig. 9 Comparison of relative sensitivity with optimum structural parameters variations for n = 1.354.

On the other hand, we have examined that wavelength (λ) verses relative sensitivity increases in the wide range of wavelength and vice versa, which is more convenience for the fiber sensor fabrication. The main obstruction is to fabricate such a complex photonic crystal fiber sensor. But the massive achievement occurs in different technological sectors. By the progression of the technological achievement, numerous fabrication techniques such as stack and draw process [38], extrusion [39], drilling [40], sol gel casting [41], and die cast process [42] have been proposed. The stack and draw process is generally preferable for honey comb and triangular lattices. It has some limitations to construct the circular pattern. Different background materials are recently used to fabricate PCF. Some of these materials are fragile. For material fragility, the drilling technique is not allowed. Extrusion is another well-known fabrication technique for soft glass nevertheless wastage of material. For design flexibility and adaptive large scale manufacturing capability, the sol gel technique helps fabricate different micro-structure PCFs. So with the help of sol gel technique, the proposed P-OPCF can be fabricated easily without any damages.

5. Conclusions

A two-layer microstructure porous cored with octagonal cladding structure inclusion with perfectly match layer (PML) has been simulated using the finite element method. In the field of electromagnetic study, the finite element method has a leading impact on analyzing and calculating the complex geometry. This study of octagonal microstructure two-layer porous core has been proposed in favor of chemical sensing. The relative sensitivity and confinement loss have been analyzed by tuning different geometrical parameters of the proposed P-OPCF structure. The simulation is also employed to calculated sensitivity for two-, three-, and four-layer porous core. It shows that the proposed micro-cored two-layer structures reflect a higher level of sensitivity 67.66 % and a low confinement loss 3.28×10^{-11} dB/m at the 1.33 μm for ethanol (RI=1.354). In fiber optics communication, wavelength band O+S+C+L is extensively used. Bearing with the wavelength band, the proposed fiber optic sensor can be applied in the wide range of wavelength (0.80 μm to 2.0 μm). Hence, it is vivid, and we confide that our designed P-OPCF will be very efficient for sensing application in the area of optical systems.

Acknowledgment

The authors are grateful to all of the subjects who participated in this research.

References

[1] X. Sang, P. L. Chu, and C. Yu, "Applications of nonlinear effects in highly nonlinear photonic crystal fiber to optical communications," *Optical and Quantum Electronics*, 2005, 37(10): 965–994.

[2] K. P. Hansen, "Introduction to nonlinear photonic crystal fibers," *Journal of Optical and Fiber Communications Reports*, 2005, 2(3): 226–254.

[3] A. Ortigosa-Blanch, J. C. Knight, W. J. Wadsworth, J. Arriaga, B. J. Mangan, T. A. Birks, *et al*., "Highly birefringent photonic crystal fibers," *Optics Letters*, 2000, 25(18): 1325–1327.

[4] T. P. Hansen, J. Broeng, S. E. Libori, E. Knudsen, A. Bjarklev, J. R. Jensen, *et al*., "Highly birefringent index-guiding photonic crystal fibers," *IEEE Photonics Technology Letters*, 2001, 13(6): 588–590.

[5] G. An, S. Li, X. Yan, X. Zhang, Z. Yuan, and Y. Zhang, "High-sensitivity and tunable refractive index sensor based on dual-core photonic crystal fiber," *Journal of the Optical Society of America B*, 2016, 33(7): 1330–1334.

[6] W. Qianet, C. L. Zhao, S. He, X. Dong, S. Zhang, Z. Zhang, *et al*., "High-sensitivity temperature sensor based on an alcohol-filled photonic crystal fiber loop mirror," *Optics Letters*, 2011, 36(9): 1548–1550.

[7] S. Olyaee and F. Taghipour, "Ultra-flattened dispersion hexagonal photonic crystal fiber with low confinement loss and large effective area," *IET Optoelectronics*, 2012, 6(2): 82–87.

[8] Aihan-Yin and L. Xiong, "Highly nonlinear with low confinement losses square photonic crystal fiber based on a four-hole unit," *Infrared Physics & Technology*, 2014, 66(9): 29–33.

[9] K. Kishor, R. K. Sinha, and A. D. Varshney, "Experimental verification of improved effective index method for endlessly single mode photonic crystal fiber," *Optics and Lasers in Engineering*, 2012, 50(2): 182–186.

[10] H. Ademgil and S. Haxha, "Endlessly single mode photonic crystal fiber with improved effective mode area," *Optics Communications*, 2012, 285(6): 1514–1518.

[11] T. A. Birks, J. C. Knight, and P. S. J. Russell, "Endlessly single-mode photonic crystal fiber," *Optics Letters*, 1997, 22(13): 961–963.

[12] M. Morshed, M. H. Imran, T. K. Roy, M. S. Uddin, and S. M. A. Razzak, "Microstructure core photonic crystal fiber for gas sensing applications," *Applied Optics*, 2015, 54(29): 8637–8643.

[13] M. Tonouchi, "Cutting-edge terahertz technology," *Nature Photonics*, 2007, 1(2): 97–105.

[14] J. M. Dudley and J. R. Taylor, "Ten years of nonlinear optics in photonic crystal fiber," *Nature Photonics*, 2009, 3(2): 85–90.

[15] N. Skivesen, A. Têtu, M. Kristensen, J. Kjems, L. H. Frandsen, and P. I. Borel, "Photonic-crystal waveguide biosensor," *Optics Express*, 2007, 15(6): 3169–3176.

[16] Y. L. Hoo, W. Jin, C. Shi, H. L. Ho, D. N. Wang, and

S. C. Ruan, "Design and modeling of a photonic crystal fiber gas sensor," *Applied Optics*, 2003, 42(18): 3509–3515.

[17] A. M. Cubillaset, S. Unterkofler, T. G. Euser, B. J. Etzold, A. C. Jones, P. J. Sadler, *et al*., "Photonic crystal fibers for chemical sensing and photochemistry," *Chemical Society Reviews*, 2013, 42(22): 8629–8648.

[18] S. Okaba, T. Takano, F. Benabid, T. Bradley, L. Vincetti, Z. Maizelis, *et al*., "Lamb-Dicke spectroscopy of atoms in a hollow-core photonic crystal fiber," *Nature Communications*, 2014, 5(5): 4096–4105.

[19] P. C. Ashok, R. F. Marchington, P. Mthunzi, T. F. Krauss, and K. Dholakia, "Optical chromatography using a photonic crystal fiber with on-chip fluorescence excitation," *Optics Express*, 2010, 18(6): 6396–6407.

[20] S. Roy, "Fiber optic sensor for determining adulteration of petrol and diesel by kerosene," *Sensors and Actuators B: Chemical*, 1999, 55(2–3): 212–216.

[21] P. N. Prasad, *Introduction to biophotonics*. New York, United States: Wiley-Interscience, 2003.

[22] L. V. Doronina-Amitonova, V. F Il'ya, O. I. Ivashkina, M. A. Zots, A. B. Fedotov, K. V. Anokhin, *et al*., "Photonic-crystal-fiber platform for multicolor multilabel neurophotonic studies," *Applied Physics Letters*, 2011, 98(25): 253706-1–253706-3.

[23] H. Shafiee, E. A. Lidstone, M. Jahangir, F. Inci, E. Hanhauser, T. J. Henrich, *et al*., "Nanostructured optical photonic crystal biosensor for HIV viral load measurement," *Scientific Reports*, 2014, 4(6174): 1032–1035.

[24] S. C. Buswell, V. A. Wright, J. M. Buriak, V. Van, and S. Evoy, "Specific detection of proteins using photonic crystal waveguides," *Optics Express*, 2008, 16(20): 15949–15957.

[25] P. Sharma and P. Sharan, "Design of photonic crystal-based biosensor for detection of glucose concentration in urine," *IEEE Sensors Journal*, 2015, 15(2): 1035–1042.

[26] H. Ademgil, "Highly sensitive octagonal photonic crystal fiber based sensor," *Optik–International Journal for Light and Electron Optics*, 2014, 125(20): 6274–6278.

[27] J. N. Dash and R. Jha, "Graphene-based birefringent photonic crystal fiber sensor using surface plasmon resonance," *IEEE Photonics Technology Letters*, 2014, 26(11): 1092–1095.

[28] B. Temelkuran, S. D. Hart, G. Benoit, J. D. Joannopoulos, and Y. Fink, "Wavelength-scalable hollow optical fibers with large photonic bandgaps for CO_2 laser transmission," *Nature*, 2002, 420(6916): 650–653.

[29] S. Atakaramians, K. Cook, H. Ebendorff-Heidepriem, J. Canning, D. Abbott, and T. M. Monro, "Cleaving of extremely porous polymer fibers," *IEEE Photonics Journal*, 2009, 1(6): 286–292.

[30] P. Yeh, A. Yariv, and E. Marom, "Theory of Bragg fiber," *Journal of the Optical Society of America*, 1978, 68(9): 1196–1201.

[31] P. Russell, "Photonic crystal fibers," *Science*, 2003, 299(5605): 358–362.

[32] J. C. Knight, T. A. Birks, P. S. J. Russell, and D. M. Atkin, "All-silica single-mode optical fiber with photonic crystal cladding," *Optics Letters*, 1996, 21(19): 1547–1549.

[33] K. Ahmed and M. Morshed, "Design and numerical analysis of microstructured-core octagonal photonic crystal fiber for sensing applications," *Sensing and Bio-Sensing Research*, 2016, 7: 1–6.

[34] T. Rylander and J. M. Jin, "Perfectly matched layer for the time domain finite element method," *Journal of Computational Physics*, 2004, 200(1): 238–250.

[35] G. Ghosh, "Sellmeier coefficients and dispersion of thermo-optic coefficients for some optical glasses," *Applied Optics*, 1997, 36(7): 1540–1546.

[36] S. Asaduzzaman, K. Ahmed, M. F. H. Arif, and M. Morshed, "Application of microarray-core based modified photonic crystal fiber in chemical sensing," in *International Conference on Electrical & Electronic Engineering*, Bangladesh, Nov. 4–6, 2015.

[37] M. S. Habib, M. S. Habib, S. M. A. Razzak, and M. A. Hossain, "Proposal for highly birefringent broadband dispersion compensating octagonal photonic crystal fiber," *Optical Fiber Technology*, 2013, 19(5): 461–467.

[38] D. Pysz, I. Kujawa, R. Stępień, M. Klimczak, A. Filipkowski, M. Franczyk, *et al*., "Stack and draw fabrication of soft glass microstructured fiber optics," *Bulletin of the Polish Academy of Sciences Technical Sciences*, 2014, 62(4): 667–682.

[39] H. Ebendorff-Heidepriem and T. M. Monro, "Extrusion of complex performs for microstructured optical fibers," *Optics Express*, 2007, 15(23): 15086–15092.

[40] S. Liu, L. Jin, W. Jin, D. Wang, C. Liao, and Y. Wang, "Structural long period gratings made by drilling micro-holes in photonic crystal fibers with a femtosecond infrared laser," *Optics Express*, 2010, 18(6): 5496–5503.

[41] H. H. El, Y. Ouerdane, L. Bigot, G. Bouwmans, B. Capoen, A. Boukenter, *et al*., "Sol-gel derived ionic copper-doped microstructured optical fiber: a potential selective ultraviolet radiation dosimeter," *Optics Express*, 2012, 20(28): 29751–29760.

[42] G. Y. Zhou, Z. Y. Hou, S. G. Li, and L. T. Hou, "Fabrication of glass photonic crystal fibers with a die-cast process," *Applied Optics*, 2006, 45(18): 4433–4436.